

**PŘÍRODOVĚDECKÁ FAKULTA
UNIVERZITA PALACKÉHO
OLOMOUC**



BAKALÁŘSKÁ PRÁCE

Michal Juhaňák
2008

PŘÍRODOVĚDECKÁ FAKULTA
UNIVERZITA PALACKÉHO
OLOMOUC

Katedra Optiky



**Experimental realization of trap detector
with single-photon sensitivity**

Bakalářská práce

Autor:

Michal Juhaňák

Studijní program:

B1701 Fyzika

Studijní obor:

Aplikovaná fyzika

Forma studia:

prezenční

Vedoucí práce:

Mgr. Miroslav Ježek Ph. D.

Termín odevzdání práce:

.....

Bibliografická identifikace

Autor: Michal Juhaňák

Název práce: Experimental realization of trap detector with single-photon sensitivity

Typ práce: Bakalářská práce

Pracoviště: Katedra optiky

Vedoucí práce: Mgr. Miroslav Ježek Ph. D.

Rok obhajoby práce: 2008

Abstrakt:

Je navržen a zkonstruován fotodetektor s jednofotonovou citlivostí využívající techniky geometrie zachycující světlo. Ztráty v důsledku odrazu na použitém jednofotonovém detekčním modulu PerkinElmer jsou minimalizovány zachycením a navrácením odraženého svazku zpět na aktivní plochu detektoru. Je pozorován nárůst detekční účinnosti detektoru cca. 11% vzhledem k účinnosti původní. Experimentální výsledky jsou porovnány s teoretickým modelem.

Klíčová slova: geometrie zachycující světlo, detektor v geometrii zachycující světlo, optický izolátor, detekční účinnost, faktor navýšení

Počet stran: 16

Jazyk: Anglický

Bibliographical identification

Author: Michal Juhaňák

Title: Experimental realization of trap detector with single-photon sensitivity

Type of thesis: Bachelor thesis

Department: Department of Optics

Supervisor: Mgr. Miroslav Ježek Ph. D.

The year of presentation: 2008

Abstract:

The photodetector with single-photon sensitivity using light-trapping geometry is designed and experimentally developed. The losses due to reflection on single-photon counting module from PerkinElmer are decreased by trapping the reflected light and tracing it back to the detector. The improvement of about 11% in number of detected photons is observed and compared with the theoretical model.

Keywords: trap geometry, trap detector, optical isolator, detection efficiency, improvement factor

Number of pages: 16

Language: English

FACULTY OF NATURAL SCIENCES
PALACKY UNIVERSITY
OLOMOUC

Department of Optics

**Experimental realization of trap detector
with single-photon sensitivity**

Michal Juhaňák
2008

Acknowledgement

I would like to thank my supervisor Mgr. Miroslav Ježek, Ph.D. for his encouragement and very helpful comments during solving both experimental and theoretical problems.

Statement

I wrote this work on my own, under supervision of Mgr. Miroslav Ježek, Ph.D, using the resources listed in the reference section.

Contents

1	Introduction	1
2	Characterization of optical components	2
3	Single-photon detector	4
4	Trap detector	5
4.1	Trap detector geometry using optical isolator.....	6
4.2	Noncollinear trap detector geometry.....	9
5	Summary and outlook	11
A	Measured values	12
B	Properties of SPCM-AQR-14 detector	13
C	Photodocumentation	14
	References	16

1. Introduction

In the last two decades the number of applications of single-photon detection increases rapidly. The remarkable evolution of information processing based on modern quantum communication and computation protocols challenges detecting devices with high quantum efficiency. The well-known protocols such quantum cryptography, quantum teleportation, entanglement swapping and others have been experimentally realized using nonclassical multiphoton states [1-4]. If N denotes number of employed photons carrying the information content and η denotes the quantum efficiency of used photodetectors then the total success rate of the protocol is proportional to the value of η^N . The several percent particular improvement of η can yield the significant increasing of the total success rate and signal-to-noise ratio [5]. Single-photon detection with low dark-count noise and high detection efficiency may allow a high-bit-rate quantum key distribution, high-speed teleportation and entanglement swapping.

The intrinsic quantum efficiency of Si and InGaAs photodetector materials reaches the value above 98%, however, the detection efficiency of commercially used single-photon counting modules varies from 15% to 75%. The aim of the thesis is to improve the total quantum efficiency of the single-photon detector using the light trapping geometry. This technique is based on collecting the reflected part of the light beam impinging the detector and tracing it back onto detector active area. The trap detector geometry can be realized in several ways with various parameters. Two types of the trap detector geometry are designed, experimentally developed and described in details in the work.

The whole thesis can be in principle divided into two parts. The first part consists of the measurement and evaluation of the optical components properties and the review of basic information on the single-photon detector that is used in the experiment. In the second part the particular realizations of the trap detector geometries are described. The main results are briefly reviewed in the summary. The thesis is completed by photodocumentation.

2. Characterization of optical components

For our experiment it is crucial to find out and evaluate power losses of all employed optical components. Hence, in the preliminary stage of the experiment the reflectivity of the broadband dielectric mirror BB1-E03 (Thorlabs) and gold coated spherical mirror NT43-340 (Edmund Optics) and transmissivity of planoconvex lenses BPX200 and LA1172-B (Thorlabs), the aspheric lens C220TME-B (Thorlabs), quarter-wave plate 460-4415 (Eksma) and polarizing beam-splitting cube 430-0252 (Ekspla) are measured. These components have proper coatings for near-infrared spectral area.

The initial continuous-wave (CW) light beam with wavelength of 814 nm is generated by the fiber-coupled laser diode FOSS 01-S3-5/125-810-S-1 (OZ Optics) and collimated to the free space. This source is used during the whole experiment. The beam impinges the optical component and it is partially reflected and transmitted. The measurement of reflectivity or transmissivity is based on comparing the optical power P_{Out} of output beam with the power P_{In} of incident one. Optical power is measured using the power-meter FieldMaster GS with the detection head LM-2 VIS (Coherent) based on silicon photodiode. The power meter is connected to a personal computer PC via RS232 serial interface. The appropriate driver allows us to set up and control the measurement by the PC. The particular power measurement lasts two minutes and consists of 120 readings. The long integration time is used to decrease the influence of laser source power fluctuations. The mean and the standard deviation are evaluated from the acquisitions.

The broadband dielectric plate mirror BB1-E03 is designed for spectral range of 750 - 1100 nm. In this interval the reflectivity guaranteed by the manufacturer for both S and P polarization modes and angle of incidence from 0° to 45° is higher than 99%. The scheme of the setup for measuring the reflectivity of BB1-E03 mirror is shown in Figure1. Two identical mirrors are used to improve the precision of the measurement. Polarizing prism Glan-laser GL5-B (Thorlabs) is used for setting the direction of linear polarization. The reflectivity of mirror is given by $R = \sqrt{P_{\text{Out}} / P_{\text{In}}}$. It is measured for angle of incidence of 45° and for almost normal incidence for both S and P polarization modes. Mean values and standard deviations of the measurement are shown in Table 1. For all setups the reflectivity of the mirror is higher than 99.5%

	2°	45°
S-polarization	$R = (99.59 \pm 0.04)\%$	$R = (99.81 \pm 0.01)\%$
P-polarization	$R = (99.71 \pm 0.04)\%$	$R = (99.74 \pm 0.01)\%$

Table 1: The measured values of reflectivity of the broadband dielectric mirror BB1-E03 for S and P linear polarizations and for angle of incidence of 2° and 45° .

The reflectivity of spherical mirror NT43-340 is measured only for the almost normal angle of incidence. Effective focal length (E.F.L) of the mirror is 50.8 mm. The output power P_{Out} is measured at the distance of two E.F.L. where the beam has approximately the same spatial properties as the incident one. Only one mirror is used for the measurement so the reflectivity is given by $R = P_{\text{Out}} / P_{\text{In}}$. As well as in the case of the plate mirror, both S and P polarization states of incident beam (with respect to the incident plane) are studied. The reflectivities reach the values of $R_s = (96.37 \pm 0.01)\%$ and $R_p = (96.10 \pm 0.02)\%$, respectively.

The plano-convex lenses BPX200 and LA1172B with the focal length of 40.0 cm were chosen to represent the BPX and LA-B types of lenses. It is assumed that all other plano-convex lenses of these two types have the same B-type coating with the same transmissivity value. The beam impinges the lens at the normal angle. The output beam power is measured just behind the lens to minimize the spatial differences between input and output beams. The value of transmissivity is then evaluated as the ratio $T = P_{\text{Out}} / P_{\text{In}}$. Measured transmissivities of BPX200 and LA1172B lenses reach the values $T = (99.24 \pm 0.08)\%$ and $T = (99.14 \pm 0.02)\%$, respectively. The transmissivity of the quarter-waveplate 460-4415 is measured in the same way. It reaches the value of $T = (99.11 \pm 0.07)\%$.

Due to a small focal length of the aspherical lens C220TME-B ($f = 11.0$ mm) the pair of these lenses is used for its transmissivity measurement. Collimated beam impinges the first lens at the normal angle of the incidence. The second lens is situated behind the first in the beam direction at distance of two focal length. The output beam (emitted by the second lens) is collimated again and it has the same spatial properties as the initial one. The transmissivity of the lens is then given by the relation $T = \sqrt{P_{\text{Out}} / P_{\text{In}}}$. Our measured value is $T = (99.05 \pm 0.01)\%$.

The last measured optical component of this set is the polarizing beam-splitting cube PBS 430-0252 from Ekspla. It is used to separate collinear beams of two different polarizations. The transmissivity for the P-polarized beam and reflectivity for the S-polarized beam is measured. The principle of the measurement is depicted in Figure 3. The linearly polarized beam transmitted by Glan-laser polarizer impinges the PBS cube at the normal angle of incidence. The polarizer is set to transmit the horizontal polarized beam (P polarized beam in the respect to incidence plane on the splitting surface) so the almost all light that impinges the PBS passes through. The passed beam goes through the quarter-wave plate, which is set to transform the initial linear polarized beam into a circular polarized one. The retro-reflection on BB1-E03 mirror traces the beam backward on the waveplate, where the polarization is modified again. Two passages through the quarter-wave plate transform the P-polarized beam into S-polarized one. The linearly polarized beam impinges PBS again and it is deflected at the angle of 90° from its initial direction. The initial power P_{In} is measured between Glan-laser and the PBS and the transmitted beam power P_{Out} just behind the PBS. Transmissivity for the P-polarized beam is then given by $T = P_{\text{Out}} / P_{\text{In}}$. The measured value is $T = (97.81 \pm 0.09)\%$. The value of the output power is then used as the P_{In} in the measurement of the reflectivity of PBS for the S-polarized beam. The corresponding output

power P_{Out} is measured in the trace of deflected beam. The reflectivity is then given by $R = P_{Out} / (P_{In} \cdot R_M \cdot T_{QW}^2)$, where R_M denotes the reflectivity of the BB1-E03 mirror and T_{QW} the transmissivity of the quarter-wave plate. The measured value of PBS reflectivity for the S-polarized beam is $R = (96.1 \pm 0.2)\%$.

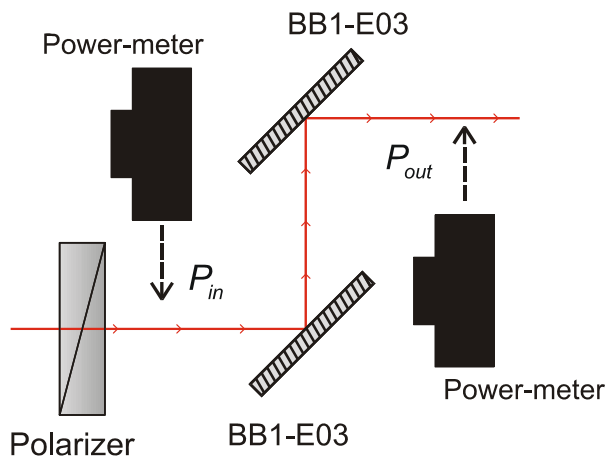
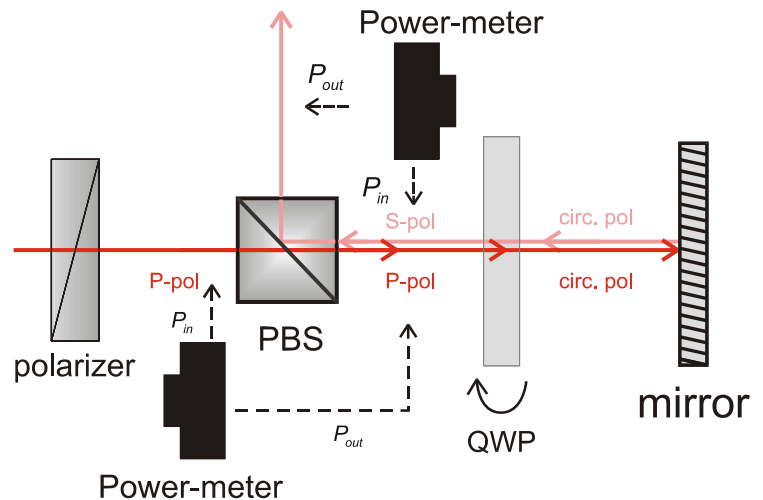


Figure 1: The scheme of the reflectivity measurement of BB1-E03 mirror.

Figure 2: The scheme of the PBS properties measurement.



3. The single-photon detector

The photodetector used in the presented experiment is the SPCM-AQR-14 manufactured by EG&G (now PerkinElmer Optoelectronics) based on silicon single-photon avalanche diode (SPAD). The operation of the SPAD is radically different to the classical APD which is more similar to a photomultiplier tube. The SPAD can generate a macroscopic current pulse in response to a single-photon incidence. It works as a bistable circuit. The diode is biased above its breakdown level but without an impinging light signal no current flows. The device is in the closed state. When photon reaches the SPAD's active area and hits some atom of the crystal grid the electron-hole pair is generated. Strong electric field accelerates generated carriers and these can impact other atoms of the crystal grid and generate secondary electron-hole pairs. The avalanche of carriers is triggered. The current then swiftly grows until the space charge

effect limits its value to a constant level. The SPAD is switched to the opened state and the macroscopic current of several miliampers can be registered. The device remains in this state until the avalanche is quenched by the external circuit back at the breakdown level (or below) and the device turns back to its initial state [6]. This process is similar to a process used in Geiger-Muller counters of ionizing radiations. Hence SPADs are also termed as Geiger-mode avalanche diodes.

The SPCM-AQR detectors are well known for their high quantum efficiency in visible and especially in near infra-red spectral area. The dependence of photon detection efficiency with respect to wavelength is shown in Appendix B. The typical value of detection probability is higher than 50% over the range from 510 to 840 nm of wavelength with a peak value higher than 70% in the area about of 700 nm. The devices use a unique SPAD called SliK, specially designed in EG&G laboratories and covered by a patent. The SliK stands for ‘Super low K’ where K denotes the ratio of the ionization coefficient of holes to that of electrons. It is a special reach-through SPAD made from ultrapure silicon with thick depletion layer of 30 μm wide. The higher thickness of depletion layer corresponds to a higher working voltage which is above 250 V. The power dissipation during the avalanche is correspondingly also high, between 5 to 10 W. To avoid the degradation or destruction of the SPCM detector, photodiode has to be thermoelectrically cooled by the Peltier cooler. The working temperature of the detector’s case should be kept between 5°C and 40°C, therefore the whole device is usually mounted onto the heat-sinking plate.

The circular active area of the SPCM-AQR-14 SliK chip has 175 μm in diameter and it is antireflection coated for visible and near infra-red spectral region. Whole diode is placed onto a gold plate and situated behind the acrylic window into a case with a shielding atmosphere. The acrylic protective window constitutes another source of the power losses due to its reflectivity. The acrylic window removed from the broken detector was available for the experiment. Its transmissivity was measured by the same way as in the case of optical components in Chapter 1. The measurement yields the value of $T_{win} = (94.02 \pm 0.01)\%$.

4. Trap detector

The probability of single photon detection by SPCM detector is about 70% at the maximum. That means the every third incident photon is lost. Principles of this could be divided into two groups. The first one is a group of intrinsic losses which includes losses during detector’s dead time, photons which goes through SliK unregistered due to a finite thickness of SliK chip depletion layer and photons absorbed by some impurities in SliK chip material which does not trigger the avalanche. The second group is formed by extrinsic losses due to the reflectivity of the detector’s parts. That means the reflectivity of SliK chip active area, the acrylic window, and the focusing lens which is the necessary part of all setups in which this device figures. The reflected photons cannot be registered, simply because they never gets into the SliK. But these photons are reflected back into a free space and some optical setup

can be used to trace them back on the active area of SliK chip. This technique is called the trap detector geometry. The simplified generic scheme of the trap geometry is illustrated in Figure 3. If η is the detection probability of the SPCM detector without trap, ρ is the reflectivity of the SPCM detector and R_{Trap} denotes reflectivity of the whole trap then the detection probability of the trap detector reads

$$\eta_{Trap} = \eta(1 + \rho R_{Trap}). \quad (1)$$

Commonly used parameter of the trap geometry is an improvement factor (I.F.). It is the ratio between the absolute count rate of the detector using the trap geometry and count the rate when trap is blocked. It is assumed that the value of detectors absolute count rate is proportional to the detection probability. Hence the improvement factor can be evaluated as

$$I.F. = \frac{\eta_{Trap}}{\eta} = 1 + \rho R_{Trap}. \quad (2)$$

The improvement factor is useful parameter in the energetic analysis of the trap geometry setup.

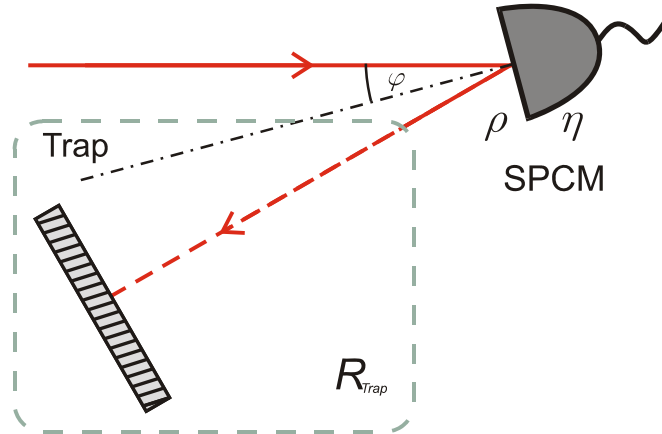


Figure 3: Simplified block scheme of the trap detector geometry.

4.1. The trap detector geometry using optical isolator

The principle of the optical isolator is outlined in Chapter 1. The measurement of the normal reflectivity of SPCM detector and the collinear trap detector geometry are realized using the described technique. The experimental setup is outlined in Figure 4. The continuous-wave light signal with wavelength of 814 nm is generated by laser diode FOSS 01-S3-5/125-810-S-1 (OZ Optics) and coupled into the single-mode optical fiber. The beam is coupled out to the free space and collimated by the aspherical lens C220TME-B (Thorlabs) with focal length of 11.0 mm. Then the beam is linearly polarized by Glan-laser polarizer and impinges the PBS at

normal angle of incidence. The polarizing beam-splitter separates the S and P components of impinging beam with a respect to a plane of incidence onto the PBS splitting surface. If the polarizer is set to transmit the P-polarized light, the almost all output power passes through PBS. Then the beam impinges the quarter-wave plate (QWP). The QWP is set to modify the linear P polarization of the beam into a circular one. Due to relatively wide beam diameter of 2.2 mm with a respect to SliK chip active area diameter of $175\ \mu\text{m}$ the proper lens has to be used for focusing. The plano-convex lens BPX060 with focal length of 50.0 mm is chosen to ensure a sufficiently tight focus. The SPCM-AQR-14 detector (serial number 4510) situated in the position of the beam waist reflected the beam back along its initial way with a same spatial properties. Two passages through the QWP turns the initial P-polarized beam in ortogonal S-polarized one. When S-polarized beam impinges the splitting surface of the PBS and it is deflected at the angle of 90 degrees from its initial direction. The retroreflecting mirror M1 is set to reflect the beam back onto SPCM detector.

Reflectivity of the SPCM detector is measured in the same way as it was described in Chapter 1 by comparing of output and input optical power. The detector is situated onto a special mount that allows a precise adjusting in two directions perpendicular to the direction of beam propagation. Because the reflectivity is not constant over the active area of the SliK chip the minimum reflectance position was used for the measurement. It is assumed that most of the impinged light is absorbed and registered by the SPCM detector at this spot. The input optical power P_{In} is detected in the position between quarter-wave plate and the plano-convex lens and corresponding output power P_{Out} before the incidence of the reflected light on the mirror M1. The net reflectivity ρ of SPCM is given by

$$\rho = \frac{P_{\text{Out}}}{P_{\text{In}} (T_{\text{QWP}} \cdot R_{\text{PBS}} \cdot T_{\text{Lns}}^2)} \quad (3)$$

where T_{QWP} denotes the transmissivity of QWP, R_{PBS} the reflectivity of the PBS and T_{Lns} the transmissivity of plano-convex lens. The reflectivity of the detector SPCM-AQR-14 reaches the value of $\rho = (7.13 \pm 0.03)\%$.

Using known reflectivities and transmissivities of individual components the analysis of light power propagation through the setup can be made. The improvement factor I.F. is given by the equation (2). The reflectivity of whole trap can be evaluated as

$$R_{\text{Trap}} = R_{\text{Mir}} (T_{\text{Lns}} T_{\text{QWP}} R_{\text{PBS}})^2 \quad (4)$$

By inserting the previous relation into (2) the improvement factor can be computed as

$$I.F. = 1 + \rho R_{\text{Trap}} = 1 + \rho R_{\text{Mir}} (T_{\text{Lns}} T_{\text{QWP}} R_{\text{PBS}})^2 \quad (5)$$

Then the I.F. factor reaches the value of $I.F. = (1.063 \pm 0.001)$ for the measured detector.

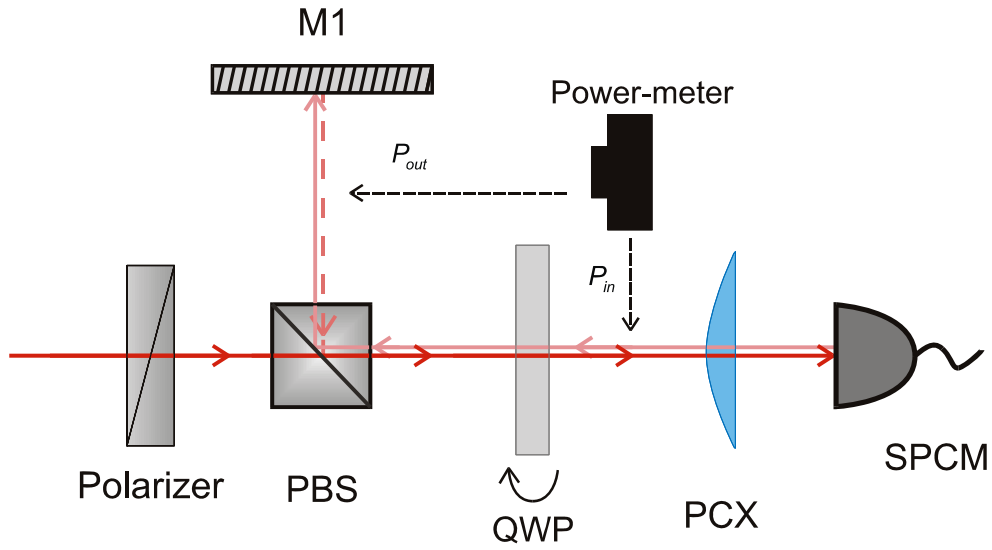


Figure 4: The setup scheme of trap detector geometry with an optical isolator used for measurement of the SPCM detector normal reflectivity.

Experimental verification of the improvement factor value is realized by measuring of the count rate with attenuated signal with and without the trap. Due to a high output power of used laser diode about 1 mW two attenuators are coupled between the source and the output coupler. They are used to set the power to the acceptable single-photon level. The measurement proceeds in the extremely low-light conditions. Detector is supplied by laboratory power supply HM 7042-5 (Hameg Instruments) and connected to the counter 974 (Ortec). The attenuators are set to ensure a mean count rate value about 10^5 counts per second with the trap blocked. The spot of the impinging beam on the SPCM detector is set in the position where the minimal reflectance was observed. The data from counter show that the position of minimum reflectance does not correspond to the maximum count rate thus the maximum sensitivity of the detector. It is considered that the minimum measured reflectance at this position is due to a beam diffusion on some impurity in the reflecting surface of the SliK chip.

The beam is set to the position where the maximal value of count rate with blocked trap is reached. Then the trap is unblocked and the mirror M1 is set to obtain the maximum count rate using the trap. The counter is connected to a personal computer via RS232 serial interface. The particular measurement lasts 10 seconds and consists of 10 readings. The dark counts are measured for both cases with and without trap separately. The table with the measured values is shown in Appendix A. The mean values and standard deviations are evaluated from the acquisitions. The improvement factor computed from the count rate measurement reaches the value of $I.F. = (1.115 \pm 0.003)$.

Finally the SPCM detector reflectivity is measured again at the same position as in the case of the maximum count rate measurement. The net value reaches $\rho = (13.1 \pm 0.1)\%$ and the corresponding improvement factor reaches the value of $I.F. = (1.116 \pm 0.002)$.

The improvement factor measured using strong signal agrees very well with the value obtained at single-photon level. The measurement yields the gain of 11.6% in count rate and thus improvement of about 7% in quantum efficiency of the particular SPCM detector.

4.2. Noncollinear trap detector geometry

The noncollinear trap detector geometry is studied using the attenuated signal. Scheme of the setup is shown in Figure 5. The laser diode with optical power of about 1 mW is coupled into the single-mode optical fiber. Two attenuators At1 and At2 are used to set the beam power at the single-photon level. The signal is coupled out and collimated into free space. The plano-convex lens BPX060 with focal length $f = 50$ mm ensures the proper focus on SliK chip active area. Beam impinges the detector at the angle of incidence of 17 degree. The reflected beam is collected by the gold coated spherical mirror NT43-340 (Edmund Optics) with effective focal length E.F.L.=50.8 mm. The mirror is situated at the distance of two focal lengths in the direction of reflected beam. The mirror is mounted in a tip-tilt mount which allows us to trace the beam back onto the SPCM detector precisely.

The setup is approximately adjusted using the strong signal under a normal light condition in the laboratory. The initial impinging beam spot and the spot of the retro-reflected beam are verified by IR-viewer and traced to the area of Slik chip. The final alignment is made in the almost absolute dark using the measured data from SPCM detector connected to a counting electronics. The beam is blocked by a beam-stop and no signal impinges the SliK chip. The dark-counts and surrounding stray light produce about 150 counts per second. Attenuators are closed totally and the beam-stop is removed. Then the attenuators are set to ensure the mean count-rate value about 10^5 counts per second with trap retro-reflector blocked. The beam is set to position where the maximum count rate is reached. Then the trap is unblocked. The maximum count rate is searched again by setting the retro-reflecting mirror M1. During the setting two peak values of count rate are observed. That means that the components of the reflected beam from the SliK chip and from the acrylic window are separated and could not be traced back on the SliK chip active area together using this particular retro-reflecting mirror and angle of incidence. Improvement factor for measured peaks yields values of 1.054 and 1.033.

The measured values are not the final ones. The experiment is still in progress. The retroreflector mirror with shorter E.F.L. will be used and the angle of incidence will be reduced by using the smaller mounts for plano-convex lens and other components. It will decrease the spacing between spatially separated reflected beams. The development of proper model for the propagation of Gaussian beams reflected on SPCM surfaces is in progress.

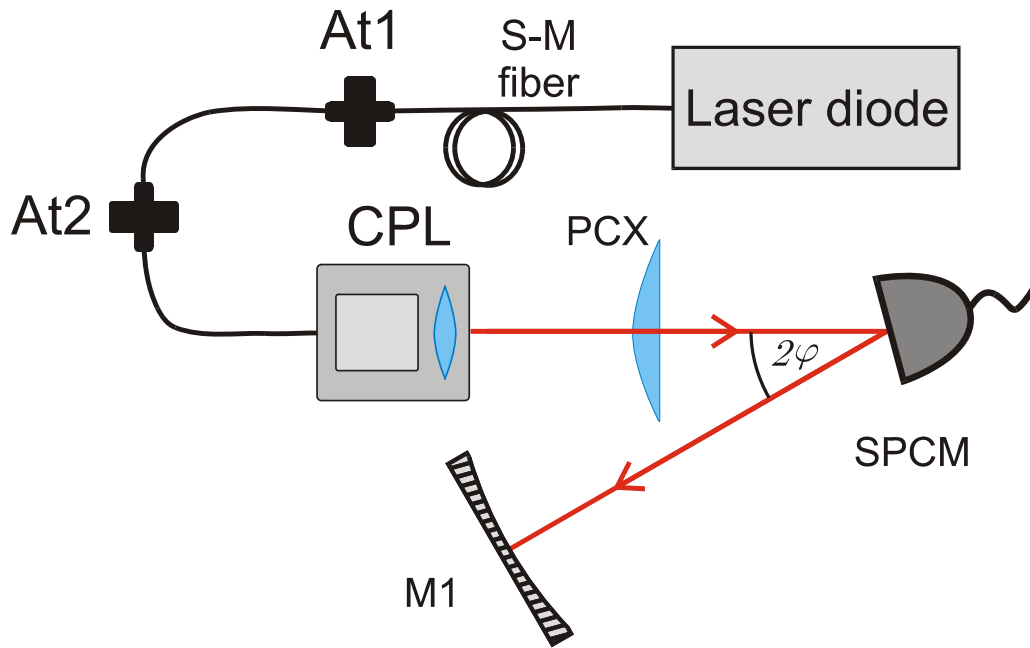


Figure 5: Scheme of noncollinear trap detector geometry. The At1 and At2 denote the attenuators, CPL means the output coupler, PCX denotes the plano-convex lens, and M1 is retro-reflecting mirror.

5. Summary and outlook

The goal of this experimental thesis was to design and build the efficient single-photon trap detector using the counting module SPCM-AQR-14 with SliK type silicon chip. The two types of trap detector geometry have been tested and described in the work.

The trap detector geometry designed for the normal angle of incidence using the optical isolator has been described. Attenuated light impinges the SPCM detector. Reflected light is traced by the optical isolator back to the active area of the detector. The count rate i.e. the number of detected photons per second has been measured. The ratio of count rates with and without retro-reflector characterizes the improvement. **The improvement factor of this geometry obtained by the count rate measurement has reached value of $I.F. = (1.115 \pm 0.003)$.** The value of improvement factor obtained by the energetic model using the detector reflectivity measurement with strong light signal agrees very well with the value acquired by the count rate measurement with single-level signal. The geometry can be used only for applications working with linearly polarized light with a fixed direction of polarization. However, the collinear geometry with normal angle of incidence allows us to trace back easily all the reflected signal. Furthure, it has been shown that the optical isolator setup can be successfully used for the measurement of normal reflectivity at the microscopic scale.

The noncollinear trap geometry has been measured by attenuated light signal too. Due to small number of employed components this setup is relatively compact with a low power losses. During the measurement two separated reflections from the SliK chip and from acrylic window have been observed. The separated beams cannot be traced back onto active area of SliK chip together by particular used components. The separately retro-reflected beams yield the improvement factors of about 1.054 and 1.033, respectively.

Non-collinear trap detector geometry is still in progress. The angle of incidence will be reduced by using smaller plano-convex lens, retro-reflecting mirror, and corresponding mounts. It will decrease the spacing between separated reflected beams. The development of proper model for the propagation of two Gaussian beams reflected on two surfaces is in progress. It will give us the answer how precisely can be both the reflected beams traced back onto 175 μm wide active area of the SliK chip.

A Tables with measured values

	CR	DC	CR-WT	DC-WT
	103415	417	114763	450
	102619	380	115111	449
	102906	390	114865	416
	103025	372	114867	469
	103152	435	114964	424
	103122	412	114438	455
	103311	383	114761	444
	102858	409	114717	451
	102994	370	115062	436
	103009	382	114804	412
Mean value	103041	395	114835	440
Standard deviation	72	7	61	6

Table 2: The results of count rate measurement of collinear trap detector using the optical isolator. The CR denotes the count rate without trap, DC denotes dark-counts with trap blocked, CR-WT denotes count rate with trap and DC-WT corresponds to dark-counts with trap.

B Properties of SPCM-AQR-14 detector

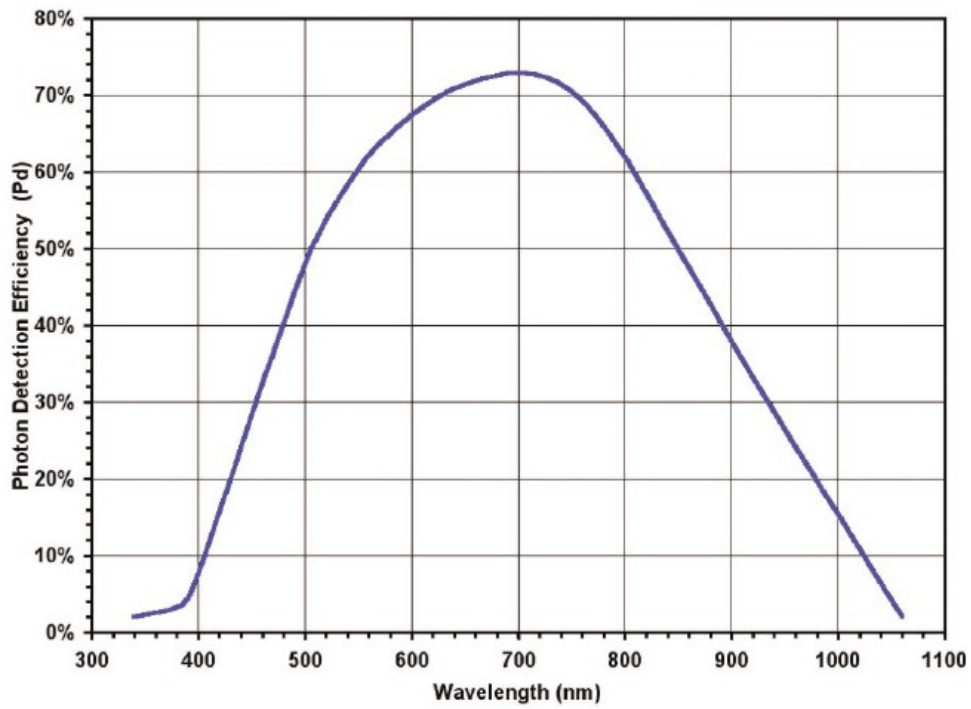


Figure 6: The photon detection efficiency of SPCM-AQR detector versus the wavelength supplied by the manufacturer (PerkinElmer). The value at 814 nm is approximately 60%.

C Photodocumentation

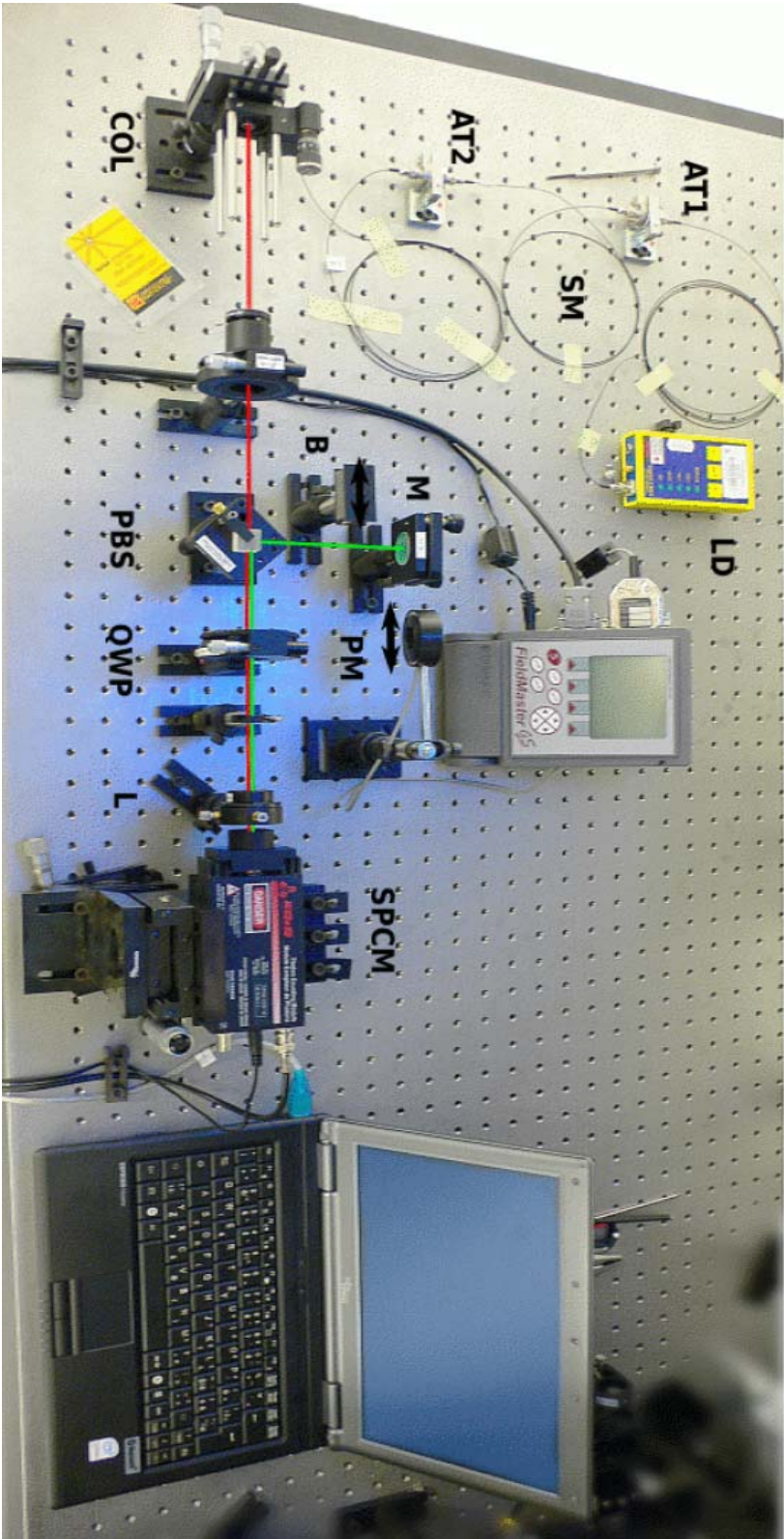


Figure 7. The setup of single-photon trap detector using the optical isolator. See text for details.

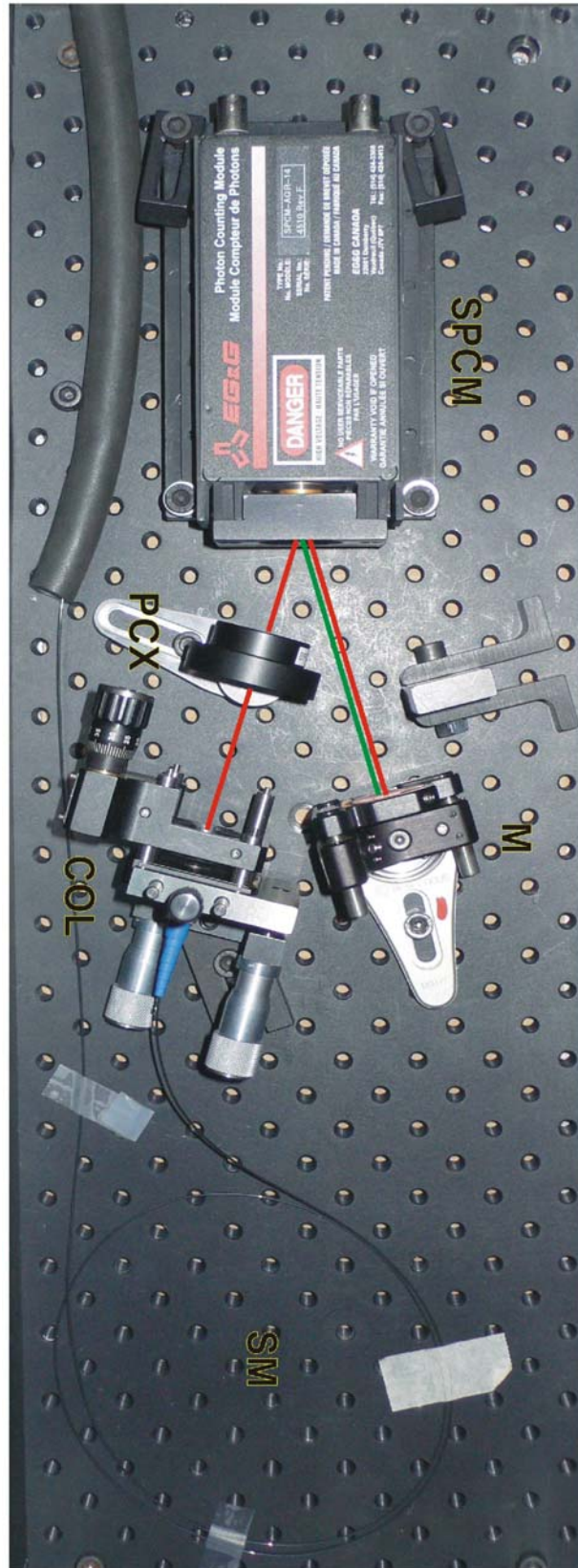


Figure 8: The setup of noncollinear trap detector. The SM denotes single-mode fiber, COL the collimator, SPCM the single-photon counting module, and M is the spherical mirror.

References

- [1] D. Bouwmeester, J. W. Pan, K. Mattle, M. Eibl, H. Weinfurter, and A. Zeilinger, Experimental quantum teleportation, *Nature (London)* **39**, 575 (1997).
- [2] J. W. Pan, D. Bouwmeester, H. Weinfurter, and A. Zeilinger, Experimental entanglement swapping: Entangling photons that never interacted, *Phys. Rev. Lett.* **80**, 3891 (1998).
- [3] D. Bouwmeester, A. K. Ekert and Anton Zeilinger, *The Physics of Quantum Information* (Springer, Berlin, 2000).
- [4] Q. Zhang, A. Goebel, C. Wagenknecht, Y.-A. Chen, B. Zhao, T. Yang, A. Mair, J. Schmiedmayer, and J.-W. Pan, Experimental quantum teleportation of a two-qubit Composite system, *Nature Physics* **2**, 678 (2006).
- [5] D. J. Jackson, G. M. Hockney, Detector Efficiency Limits on Quantum Improvement, *Journal of Modern Optics* **51**, 2429 (2004).
- [6] S. Cova, M. Ghioni, A. Lotito, I. Rech and F. Zappa, Evolution and prospects for single-photon avalanche diodes and quenching circuits, *Journal of Modern Optics* **51**, 1267 (2004).